Preparation and XPS Surface Chemical Analysis of PS/PU Nanocomposites

Yan Zhu,[1] Lian-Meng Zhang,[2] Hua Zheng,[1] Duo-Xian Sun[3]

[1]*School of Chemical Engineering and Technology, Wuhan University of Technology, Wuhan 430070, China*
[2]*State Key Laboratory of Advanced Technology for Materials Synthesis Processing, Wuhan University of Technology, Wuhan 430070, China*
[3]*School of Chemical Engineering and Technology, Tianjin University, Tianjin 300072, China*

Received 27 February 2005; accepted 16 July 2005
DOI 10.1002/app.22725
Published online in Wiley InterScience (www.interscience.wiley.com).

ABSTRACT: Aqueous emulsions of anionic polyurethane ionomers, based on polypropylene glycol as soft segment, isophorone diisocyanate as diisocyanate, dimethylolpropionic acid as chain extender and potential ionic center, and triethylamine as neutralizer, were synthesized. They were mixed with styrene monomers to prepare polystyrene–polyurethane (PS/PU) nanocomposites by an evocator. The sizes and distributions of the particles were measured by dynamic light scattering, and the microstructure of the nanocomposites was observed by transmission electron microscope. X-ray photoelectron spectroscopy (XPS) was used to study the surface characterization of anionic PU and PS/PU nanocomposites. It could be found that the nanoparticles of PU could encapsulate the styrene monomers effectively and the leakage type of every element in PU was not affected by the introduction of Ps. There were more hard segments on the surface of crosslinking PS/PU nanocomposites because of the formation of crosslinking structure and interpenetrating polymer network between PU and PS. © 2006 Wiley Periodicals, Inc. J Appl Polym Sci 100: 3889–3894, 2006

Key words: X-ray photoelectron spectroscopy; polystyrene; polyurethane; nanocomposites

INTRODUCTION

Polyurethanes (PUs) are a versatile group of multiphase segmented polymers that have excellent mechanical properties, good hardness, high abrasion, and chemical resistance.[1,2] Morphologic studies of segmented PUs have shown that these polymers separate into two phases, leading to domains composed of hard segments and domains composed mostly of soft segments.[3,4] It has also been reported that not only does the segregation take place in the bulk, but on the basis of the studies using surface analysis techniques such as X-ray photoelectron spectroscopy (XPS), the surface of these PU is enriched in the soft segments with respect to the bulk composition of the polymers.[5–10]

According to the conclusion suggested by Lorenz,[11,12] anionic PU ionomers in water are stabilized because of electric double layer and solvent effect. Because the soft segment of anionic PU is hydrophobic and hard segment with COO^{-} is hydrophilic, the molecule chains of anionic PU can self-organize to micelles when it is dispersed in water. The hydrophilic groups in the micelles are on the surfaces of particles and hydrophobic groups are crimped into the particles as showed in Figure 1.[13] The micelles make a Brownian motion and negative charges are simultaneous with positive ones, and so an electric double layer is formed on the surface of the particles and there is a voltage between them. The voltage blocks the gathering of particles and makes them act as a surfactant. At the same time, there are hydrogen bonds between the hydrophilic groups and water molecules, and then the particles are surrounded by a layer of water molecules. The solvent effect can also hinder the gathering of particles. In this study, particles with a dimension in the 10–100 nm range were used to encapsulate styrene monomers, and polystyrene was synthesized by an evocator. At last, anionic polystyrene/polyurethane (PS/PU) nanocomposite dispersions of core-shell-type were prepared in situ.

The surface analysis of polymers can now rely on many spectroscopic techniques,[14–19] some of them being well established. XPS is probably one of the most popular and accessible methods to analyze the surface chemistry of materials. To the best knowledge of present authors, there is little information about surface analysis of anionic PU ionomers and their nanocomposites by XPS.

In this work, uncrosslinking and crosslinking PS/PU nanocomposites were prepared. The exact distribution of soft and hard segments of PU near the very top surface was precisely known by XPS analysis.

Correspondence to: Y. Zhu (whlgdxzhy@sina.com).

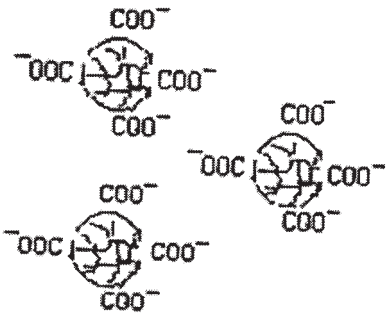

Figure 1 Micelles of anionic PU.

EXPERIMENT

Materials

Polypropylene glycol (PPG, $M_n = 1000$) (Tianjin chemical company, China), isophorone diisocyanate (IPDI) (Nuodex Inc, Japan), dimethylolpropionic acid, (DMPA) (Tianjin chemical company, China). Prior to use, IPDI was used vacuum distilled at 70°C and 0.025 mmHg. PPG was degassed at 40°C and 0.5 mmHg.

Preparation of aqueous emulsion of anionic PU ionomers

A 250 mL round-bottomed, four-necked separable flask with a mechanical stirrer, thermometer, and condenser with drying tube was used as a reactor. The reaction was carried out in a thermostat. IPDI (7.33 g) and PPG (10 g) were dissolved in HEA solvent, and then the whole solution was heated to 85°C for 3 h with stirring to form a prepolymer. Then, 2.38 g of DMPA was added to the prepolymer and kept at 85°C for 0.5 h, followed by end capping with isopropanol at 60°C for 15 min. Finally, 1.0 g triethylamine and 80 mL distilled water were added to form aqueous emulsion, after which HEA was removed by reduced pressure distillation at 45°C. The final concentration of PU in water was about 20% by weight.

Preparation of PS/PU nanocomposites

When aqueous emulsion of anionic PU ionomers was finished as described in the previous section, certain amount of styrene monomer with styrene/PU ratio of 1:1 by weight was gradually dropped into PU aqueous emulsion at 80°C for 0.5 h, followed by the addtion of hydrogen peroxide. Then the polymerization of styrene was carried out at 80°C for 4 h. At last, the aqueous emulsion of uncrosslinking PS/PU nanocomposites was formed.

When little amount of 2-butene-1,4-diol is used to replace the same amount of PPG during the preparation of aqueous emulsion of anionic PU ionomers, crosslinking PS/PU nanocomposites could be prepared.

Film preparation

The aqueous emulsions were cast onto a clean aluminum pan and allowed to evaporate overnight in an oven at 50°C. All films were about 1.0 mm thick.

Measurement

The morphology of the PS/PU nanocomposite particles was observed by a transmission electron microscope of Philips EM400ST. The sample was prepared by depositing the emulsion on a copper net after being stained by Phospho-wolframic acid.

Average sizes and size distributions of the particles in aqueous emulsions were measured by dynamic light scattering (BI9000AL), where an Ar-type laser with wavelength 514.5 nm was used. The samples were firstly diluted with deionized water to 0.5%, followed by ultrasonic wave treatment to homogenize the emulsions.

XPS was performed on a PHI1600 (PE CO. US) with a hemisphere analyzer and a position sensitive detector. The spectrometer was equipped with a Mg/Kα(1253.6 eV) achromatic X-ray source operated at a power of 250 W. The spot size used was 1×3 mm^2. Survey scans were taken in the range of 0–1100 eV. Any significant peaks in the survey scan were then subjected to narrow scans in the appropriate ranges for atomic concentration analysis. Photopeaks were curve-fitted using Origin 6.1 software to obtain information on the bonding state of the elements. Binding energies were referenced to the carbon–carbon bond that was assigned a binding energy of 285.0 eV. The spectrometer was typically run at the 5×10^{-9} Torr vacuum range.

RESULTS AND DISCUSSIONS

Figure 2 is the TEM micrographs of pure PU and PS/PU nanocomposites colored by phospho-wolframic acid. We could see clearly that the particles of pure PU were approximately round with a diameter of about 30–40 nm and size distribution was narrow, and PS/PU nanocomposites were 60–80 nm and wider. Because the colored degree of PU was different from that of PS, the core-shell structure of PS/PU nanocomposites could be seen clearly. However, the particles of crosslinking PS/PU nanocomposites deviated from round and gathered in bulk. This was because 2-butene-1,4-diol existing in soft segments could react with styrene monomers, and then the crosslinking structure and interpenetrating polymer network were formed between core and shell or particles. These could also be proved in Figure 3, measured by

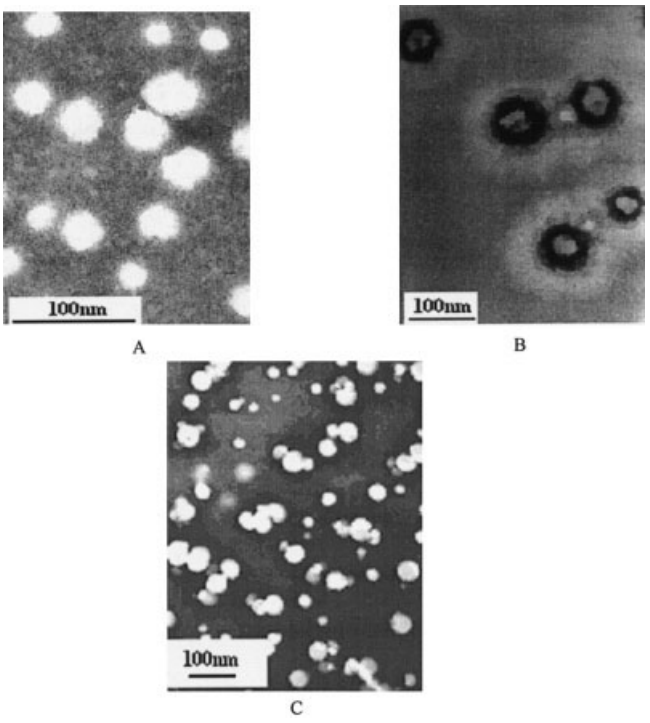

Figure 2 TEM images of PS/PU nanocomposites (100,000 times). (A) Pure PU, (B) uncrosslinking PS/PU nanocomposites, and (C) crosslinking PS/PU nanocomposites.

dynamic light scattering. The particle size of PS/PU nanocomposites was larger than that of PU, and the distribution was wider. The size actually doubled going from PU to uncrosslinking PS/PU nanoparticles.

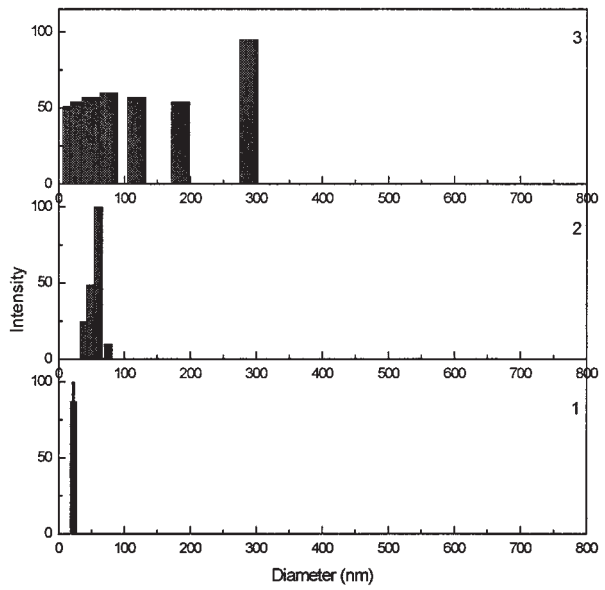

Figure 3 The sizes and distributions of PU and PS/PU nanocomposites. (1) Pure PU, (2) uncrosslinking PS/PU nanocomposites, and (3) crosslinking PS/PU nanocomposites.

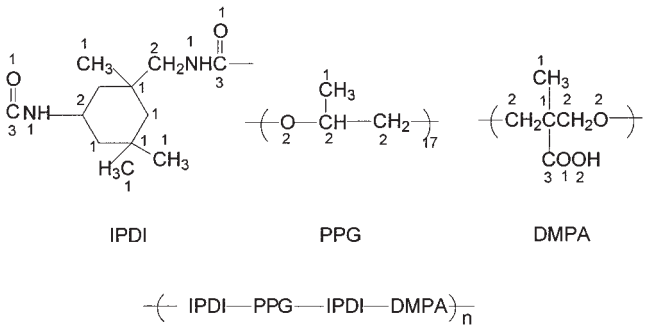

Figure 4 Chemical structure of anionic PU's components and the marks corresponding to different functional group.

This is because PU micelles could encapsulate styrene monomers effectively and supplied micro-reactors for the polymerization. The electric double layer and solvent effect would block the gathering of particles. However, because the nanoparticles were of a loose structure, existence of PS within PU nanocapsules caused the increasing particles in the diameter. As to crosslinking PS/PU nanocomposites, the crosslinking structure and interpenetrating polymer network caused gathering of particles, and then the particle size got larger and distribution wider.

The chemical structure of anionic PU's components and the marks corresponding to different functional groups were shown in Figure 4. The XPS survey spectrum of anionic PU, corresponding to carbon, nitrogen, and oxygen atoms, was detected as presented in Figure 5.

The patterns of the fitting peak treatment for the XPS spectra of C1s, O1s, and N1s in anionic PU were presented in Figure 6. High resolution spectra of signal showed an envelope that could be curve fitted into a series of peaks corresponding to different functional groups. The peak usually at the lowest binding energy

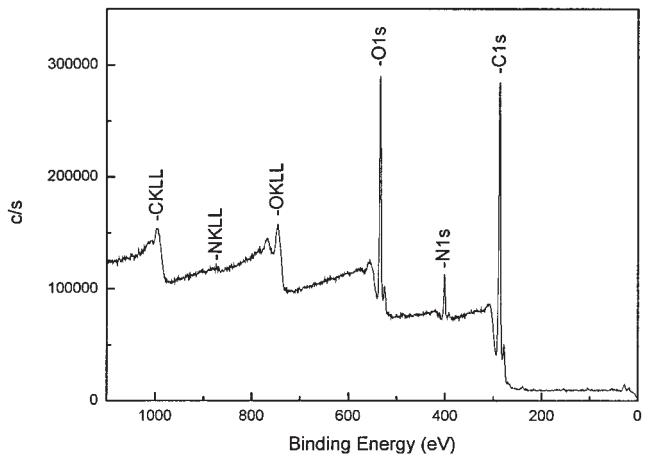

Figure 5 XPS survey spectrum of anionic PU showing the peaks corresponding to oxygen, nitrogen, and carbon atoms.

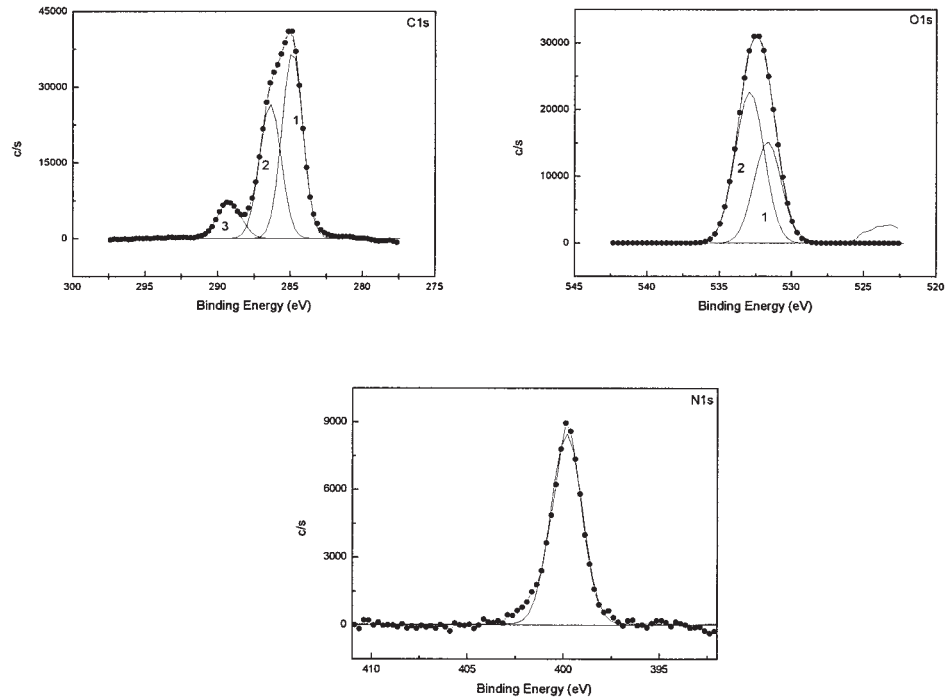

Figure 6 Pattern of the fitting peak treatment for the XPS spectra of C1s, O1s, and N1s in anionic PU.

(285.0 eV) was assigned to carbon atoms that were linked only to carbon (C—C*) and hydrogen atoms (C*—H). The peak shifted by ~1.4 eV was corresponding to carbon atom linked to one carbon or hydrogen atom and one oxygen atom via a single bond (C*—O). Carbon peaks corresponding to carbonyl O—C*═O and N—C*═O functions appeared shifted by about 4.2 eV, respectively, from the C*—C peak. We ignored secondary neighbor effects and considered C*—O and C*—N as having a similar chemical shift with respect to the C*—C peak. Similarly, the oxygen peak corresponding to carbonyl O*═C—N and O*═C—O was at 531.5 eV, and the peak shifted to 533.0 eV was corresponding to C—O*. The peak corresponding to nitrogen atoms linked to carbonyl N*—C═O was at 399.9 eV. Because the carbonyls and nitrogen atoms only existed in the hard segments of anionic PU as shown in Figure 3, the exact distribution of soft and hard segments of PU near the very top surface of PS/PU nanocomposites could be determined from them.

Table I and Figure 7 showed the results and patterns of the fitting peak treatment for the XPS spectra of uncrosslinking and crosslinking PS/PU nanocomposites. Quite similar spectrums were obtained for them but with slightly different peak intensities. However, the relative areas (%) of C1s peak at 289.2 eV and O1s peak at 531.5 eV of PS/PU nanocomposites were higher than those of PU, and the absolute area of N1s peak of crosslinking PS/PU nanocomposites (9440) was larger than that of PU (8428.5) and uncrosslinking PS/PU nanocomposites (8611.3). We can say that the chemical environment of various elements in PU was not changed by the introduction of PS as well as the formation of crosslinking structure and interpenetrating polymer network between core and shell. At the same time, the enrichment of hard segments on the surface of PU and PS/PU nanocomposites was very obvious, which was contrary to the conclusion of other researchers.[5–10] Because of the existence of PS, the amount of the hard segments on the surface of nanocomposites increased, and the increasing extent of that

TABLE I
Result of the Fitting Peak Treatment for the XPS Spectra

	C1s			O1s		N1s
	1	2	3	1	2	1
Binding energy (eV)	285.0	286.4	289.2	531.5	533.0	399.9
Area of PU (%)	50.76	37.99	10.25	38.89	61.11	100
Area of uncrosslinking PS/PU (%)	54.40	35.08	10.52	50.91	49.09	100
Area of crosslinking PS/PU (%)	58.14	33.89	10.96	56.87	43.13	100

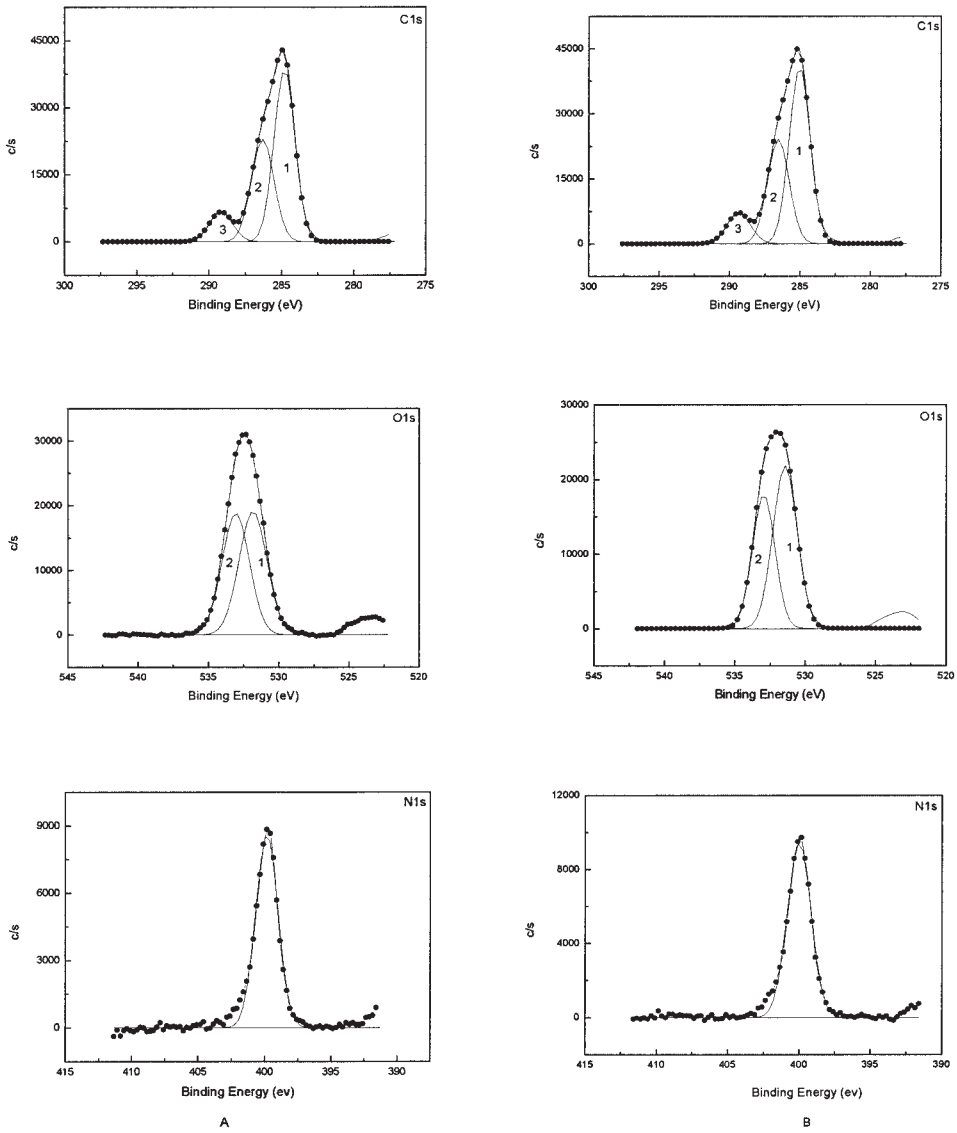

Figure 7 Pattern of the fitting peak treatment for the XPS spectra of C1s, O1s, and N1s. (A) Uncrosslinking PS/PU nanocomposites and (B) crosslinking PS/PU nanocomposites.

of crosslinking PS/PU nanocomposites was higher than those of uncrosslinking. This was because the formation of anionic PU ionomers in water made hard segments with COO^{--} shift to the surface of particles. At the same time, a polymerization between PS and 2-butene-1,4-diol in soft segments occurred and the formation of crosslinking structure and interpenetrating polymer network made more soft segments shift inside the nanoparticles.

CONCLUSIONS

In conclusion, the nanoparticles of PU could encapsulate the styrene monomers effectively, and thus PS/PU nanocomposites were prepared. The leakage type of various elements in PU was not affected by the introduction of PS. The surfaces of PU and PS/PU nanocomposites were enriched in the hard segments. There were more hard segments on the surface of crosslinking PS/PU nanocomposites because of the formation of crosslinking structure and interpenetrating polymer network between PU and PS.

References

1. Noshay, A.; McGrath, J. E. Block Copolymers: Overview and Critical Survey; Academic Press: New York, 1977; p 16–59.
2. Oertel, G. (Ed.) In Polyurethane Handbook, 2nd ed; Hanser: New York, 1993; p 22–45.
3. Cooper, S. L.; Tobolsky, A. V. J Appl Polym Sci 1966, 10, 1837.
4. Cooper, S. L.; Estes, G. M. (Eds.) In Multiphase Polymers; American Chemical Society: Washington, DC, 1979; Advances in Chemistry Series no. 176.

5. Thomas, H. R.; O'Malley, J. J. Macromolecules 1979, 12, 323.
6. O'Malley, J. J.; Thomas, H. R.; Lee, G. M. Macromolecules 1979, 12, 996.
7. Yoon, S. C.; Ratner, B. D. Macromolecules 1986, 19, 1068.
8. Yih, R. S.; Ratner, B. D. J Electron Spectrosc Relat Phenom 1981, 43, 61.
9. Schmitt, R. L.; Gardella, J. A.; Magill, J. H.; Salvati, L.; Chin, R. L. Macromolecules 1985, 18, 2675.
10. Hearn, M. J.; Ratner, B. D.; Briggs, D. Macromolecules 1988, 21, 2950.
11. Lorenz, O.; Haulena, F.; Kleben, O. A. Macromol Chem 1973, 33, 159.
12. Lorenz, O.; Hick, H. A. Macromol Chem 1978, 72, 115.
13. Macknight, W. J.; Earnest, T. R. J Polym Sci Part D: Macromol Rev 1981, 16, 41.
14. Sabbatini, L.; Zambonin, P.G. (Eds.) In Surface Characterization of Advanced Polymers; VCH, Weinheim: Germany, 1993.
15. Briggs, D. In Practical Surface Analysis, Vol. 1; Briggs, D.; Seah, M. P., Eds.; Wiley: Chichester, UK, 1990; p 437–489.
16. Briggs, D. In Practical Surface Analysis, Vol. 2; Briggs, D.; Seah, M. P., Eds.; Wiley: Chichester, UK, 1992; p 367–392.
17. Vickerman, J. C.; Brown, A.; Reed, N. H.; Secondary Ion Mass Spectrometry—Principles and Applications; Clarendon Press: Oxford, UK, 1989.
18. Gardella, J. A.; Pireaux, J. J. Anal Chem 1990, 62, 645.
19. Chou, N. J. In New Characterization Techniques for Thin Polymer Films; Ho-Ming, T.; Luu, T., Eds.; Wiley: Chichester, UK, 1990; p 289–298.